A multiscale model for dilute turbulent gas-particle flows based on the equilibration of energy concept

Ying Xu and Shankar Subramaniam

Re-register for Table of Content Alerts

Create a profile.
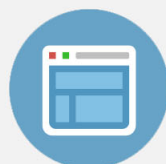
Sign up today!

A multiscale model for dilute turbulent gas-particle flows based on the equilibration of energy concept

Ying Xu[a] and Shankar Subramaniam[b]

Department of Mechanical Engineering, Iowa State University, Ames, Iowa 50011

The objective of this study is to improve Eulerian-Eulerian models of particle-laden turbulent flow. We begin by understanding the behavior of two existing models—one proposed by Simonin [von Kármán Institute of Fluid Dynamics Lecture Series, 1996], and the other by Ahmadi [Int. J. Multiphase Flow **16**, 323 (1990)]—in the limiting case of statistically homogeneous particle-laden turbulent flow. The decay of particle-phase and fluid-phase turbulent kinetic energy (TKE) is compared with direct numerical simulation results. Even this simple flow poses a significant challenge to current models, which have difficulty reproducing important physical phenomena such as the variation of turbulent kinetic energy decay with increasing particle Stokes number. The model for the interphase TKE transfer time scale is identified as one source of this difficulty. A new model for the interphase transfer time scale is proposed that accounts for the interaction of particles with a range of fluid turbulence scales. A new multiphase turbulence model—the equilibration of energy model (EEM)—is proposed, which incorporates this multiscale interphase transfer time scale. The model for Reynolds stress in both fluid and particle phases is derived in this work. The new EEM model is validated in decaying homogeneous particle-laden turbulence, and in particle-laden homogeneous shear flow. The particle and fluid TKE evolution predicted by the EEM model correctly reproduce the trends with important nondimensional parameters, such as particle Stokes number. © *2006 American Institute of Physics.* [DOI: 10.1063/1.2180289]

I. INTRODUCTION

Modeling dilute particle-laden turbulent flows is an important research topic with applications in the freeboard of fluidized beds, and in particle transport through pneumatic conveying.[1,2] Turbulence enhances the momentum, heat, and mass transfer between the dispersed phase and the carrier phase. Our focus is on solid suspensions that are low in volume fraction, but which still have relatively high mass loading due to high thermodynamic density of the particles. Since the particle volume fraction is low, the influence of particles on the carrier phase mass conservation equation is often neglected, and so are interparticle collisions. However, the particles significantly alter carrier phase turbulence; hence, "two-way" coupling needs to be taken into consideration.

It is useful to adopt a statistical description in these flows. Two commonly used modeling approaches to describe two-phase turbulent flows are the two-fluid (or Eulerian-Eulerian approach),[3] and the number-density-based Lagrangian-Eulerian approach.[4,5] In the Eulerian-Eulerian approach, flow quantities such as the velocity in each phase are averaged, and these averaged quantities are used to describe the characteristics of the carrier and dispersed-phase flow fields. This approach leads to unclosed terms representing the interaction between the phases. Once these terms are modeled to close the equation system, the Eulerian-Eulerian approach can be used in computational fluid dynamics

(CFD) calculations of multiphase flow. In this work we focus on the Eulerian-Eulerian approach.

Two popular multiphase turbulence models based on the Eulerian-Eulerian approach are reviewed here. Ahmadi[6] used the ensemble-averaging method to derive the evolution equation for TKE in the carrier and dispersed phases. The transport equation for dissipation rate in fluid phase is taken to be the standard k-ε model for single-phase turbulence. Ahmadi's model contains the specification of model constants for dilute two-phase flows and dense granular flows as special limiting cases. Validation of this model has been reported for simple shear flow of a dense mixture.[7] In this case the particle volume fraction is relatively high (>0.1) compared to the test cases described in this work (particle volume fraction $\sim 10^{-3}$). A four-equation model proposed by Simonin and co-workers[8,9] is widely used in multiphase flow calculations. It has been tested by other researchers,[10] and compared with experimental results for turbulent gas-solid flows in a vertical pipe,[1] and in a vertical riser.[2]

Eulerian-Eulerian (EE) models, such as those described here, are used in CFD codes for simulating multiphase flows in engineering applications. Typical applications include design and scaleup of circulating fluidized combustors and coal gasifiers. These CFD simulations can be improved if the turbulence model reproduces important physical phenomena such as turbulence modification with variation in particle Stokes numbers. The turbulence model should also satisfy some basic modeling and performance criteria, and must be validated in canonical turbulent particle-laden flow problems. Model validation can be performed by using direct

[a]Electronic mail: xying@iastate.edu
[b]Electronic mail: shankar@iastate.edu

18, 033301-1

numerical simulation (DNS) data or experimental data for gas-solid turbulent flows. By performing these validation tests, the prediction of multiphase flows using general purpose CFD codes can be further improved.

Direct numerical simulations of particle-fluid interaction in turbulent flows have been performed by many researchers.[11–18] The flow configurations in these studies include homogeneous turbulence (decaying and stationary), homogeneous shear flow, and plane-strain turbulence. Different aspects of the particle-phase influence on fluid turbulence have been studied using DNS, including: (i) the modification of TKE decay rate in fluid phase with increasing particle Stokes numbers;[11,12,18] (ii) the effect of mass loading on the decay rate of fluid-phase TKE;[11,12,14,15] (iii) the modification of fluid TKE spectra and fluid-phase dissipation rate due to the presence of particles.[11,12,14,16,18] These studies provide physical insight into the nature of particle-turbulence interactions, as well as data on TKE evolution in both phases. The multiscale interaction mechanism that is revealed by DNS directly motivates the development of the new EE model proposed in this work. The DNS data on TKE evolution are also used to test and validate EE models in this study. However, the validation of EE models using DNS data is limited by the quantities reported in the literature. Although direct numerical simulations[11,12,14,15,18] report the influence of particle Stokes number and mass loading on TKE of fluid and particle phase, they do not report detailed budgets of terms in the TKE and dissipation rate evolution equations. The interphase TKE transfer term, which is important for validating two-fluid EE models, is also not available from these studies.

The interaction between particles and fluid turbulence has also been studied using large eddy simulation (LES) with Lagrangian particle tracking. This approach is not so severely restricted to the range of Reynolds numbers and flow-field configurations, while DNS calculations remain restricted to relative low Reynolds numbers due to high computational cost. LES studies with Lagrangian particle tracking are used primarily to investigate one-way coupling between the fluid and particles.[19–21] In these works the effect of the velocity field (which is only partially resolved in LES) on particles is modeled. However, even for volumetrically dilute gas-solid flows the effect of two-way momentum coupling is important if the mass loading is significant. This necessitates modification of the LES subgrid model for fluid turbulence, as discussed by Squires.[22] For these reasons alone, it is not fruitful to use the predictions from LES with Lagrangian particle tracking to validate EE models or to calibrate EE model constants. Therefore, this study is focused on using DNS results to validate and improve EE models for particle-laden turbulence.

The objective of this work is to

(1) perform a comparative assessment of model predictions with direct numerical simulation data for a canonical turbulent particle-laden flow;

(2) identify modeling criteria based on this comparative assessment;

(3) propose a new multiphase turbulence model for dilute particle-laden turbulent flows, and derive the transport

equations for the Reynolds stress tensor in the fluid and particle phases; and

(4) validate this new multiphase turbulence model in canonical turbulent particle-laden flow problems, and ensure that this model satisfies the modeling criteria identified in the comparative study.

II. COMPARATIVE ASSESSMENT OF SIMONIN AND AHMADI'S MULTIPHASE TURBULENCE MODELS

An important limiting case of turbulent multiphase flows is statistically homogeneous particle-laden turbulent flow evolving in a zero-gravity environment. The principal findings from direct numerical simulations of this flow by Sundaram and Collins,[11] and the results from a comparative assessment of two multiphase turbulence models, are summarized in this section.

If gravity is absent and the mean velocity fields are homogeneous, the mean pressure gradient is zero and the mean momentum equation system results in the trivial solution of zero mean velocity in each phase, which implies a zero mean slip velocity.[5] If the flow field is initialized with zero mean velocity in both phases, the mean velocities will remain zero. In this case, it is easy to study the evolution of second moments of fluctuating velocity solely influenced by interphase TKE transfer and viscous dissipation (without effects of mean velocity gradients).

In this DNS study,[11] rigid, spherical solid particles evolve in freely decaying homogeneous turbulent flow. There is no interphase mass transfer. The flow is dilute, with particle density much larger than fluid density ($\rho_p/\rho_f \approx 10^3$). The particle size is in the sub-Kolmogorov range ($\eta = 0.035$ and $d/\eta < 1$, where d is the mean particle diameter), but the particles are large enough to ignore Brownian motion. Hence, a linear drag law can be applied to each particle in the momentum equations.

The boundary layer around each particle is neglected, and particles are viewed as point particles in the flow field. (However, kernel averaging is performed to interpolate the interphase momentum transfer to the fluid momentum equation.) Particle collisions are assumed to be elastic, so collisions conserve particle kinetic energy. Since the particle volume fraction is quite low, the influence of the particles on the fluid-phase continuity equation is neglected, but the effects on fluid momentum are still taken into account.

The predictions from DNS show that the energy in both phases decreases monotonically and the net effect of particles is to reduce fluid energy. An important nondimensional quantity that characterizes the inertia of the solid particles is the Stokes number $\mathrm{St} = \tau_p/\tau_f$, which is defined as the ratio of the characteristic particle momentum response time $\tau_p = (\rho_p/\rho_f)d^2/18\nu_f$ to a characteristic flow time scale τ_f. In Sundaram and Collins' DNS study,[11] the characteristic flow time scale is chosen to be the Kolmogorov time scale $\tau_\eta = (\nu/\varepsilon)^{1/2}$, and therefore the Stokes number in this work is defined as $\mathrm{St} \equiv \tau_p/\tau_\eta$. DNS results[11] show that the effect of the particles to reduce fluid energy grows with increasing particle Stokes number. The particle energy also decays
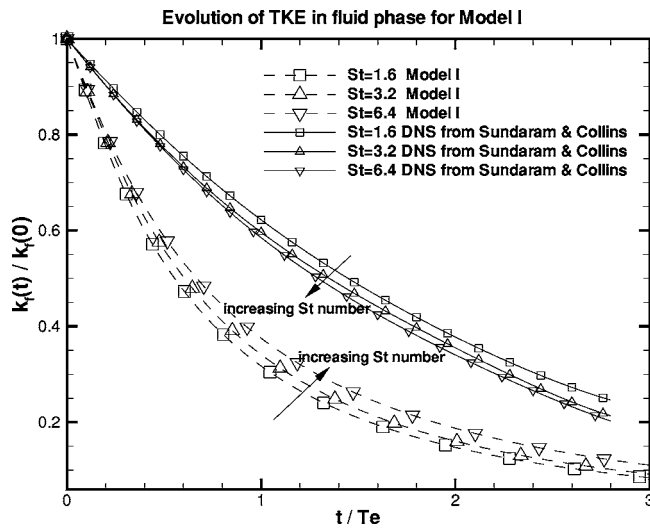
FIG. 1. Evolution of TKE in fluid phase from model I for decaying homogeneous particle-laden turbulent flow. Arrows in the figure indicate the direction of increasing particle Stokes number.

monotonically in time, and the decay rate increases with increasing particle Stokes number (for fixed mass loading). See the solid lines in Figs. 1 and 2.

We now summarize the two multiphase turbulence models that are used to predict the decay of kinetic energy in the decaying homogeneous turbulence case described above. Hereafter, Simonin's model is referred to as model I in this work, and Ahmadi's model is referred to as model II.

A. Model I—Simonin's model: Model description and results

For decaying homogeneous particle-laden turbulent flow, the simplified model equations for TKE and dissipation rate in fluid phase from model I[8,9] are
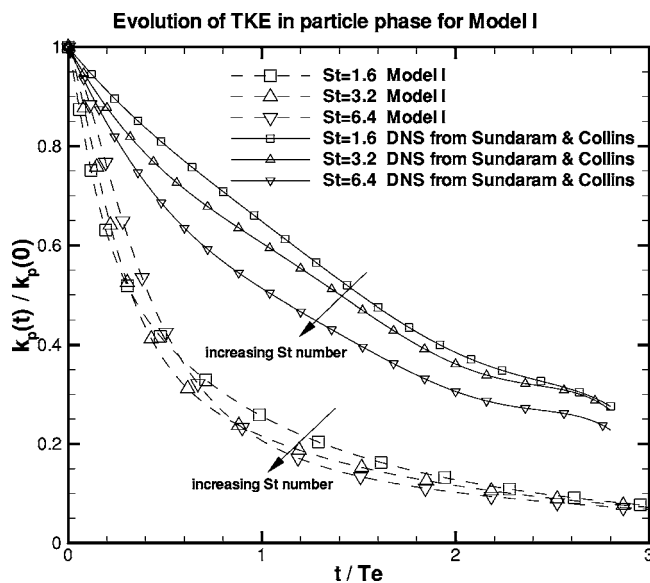

FIG. 2. Evolution of TKE in particle phase from model I for decaying homogeneous particle-laden turbulent flow.

$$\alpha_f \rho_f \frac{dk_f}{dt} = \Pi_{k_f} - \alpha_f \rho_f \varepsilon_f, \tag{1}$$

$$\alpha_f \rho_f \frac{d\varepsilon_f}{dt} = C_{\varepsilon,3} \frac{\varepsilon_f}{k_f} \Pi_{k_f} - \alpha_f \rho_f C_{\varepsilon,2} \frac{\varepsilon_f^2}{k_f}, \tag{2}$$

where $C_{\varepsilon,2} = 1.92$ and $C_{\varepsilon,3} = 1.2$. The particle-phase influences fluid-phase TKE through the interphase TKE transfer term $\Pi_{k_f} = \alpha_p \rho_f F_D [k_{fp} - 2k_f]$, where F_D plays the role of an effective particle response frequency.

The model transport equation for TKE in particle phase simplifies to

$$\alpha_p \rho_p \frac{dk_p}{dt} = \Pi_{k_p} = -\alpha_p \rho_p \frac{1}{\tau_{12}^F} [2k_p - k_{fp}], \tag{3}$$

$$\alpha_p \rho_p \frac{dk_{fp}}{dt} = \Pi_{k_{fp}} - \alpha_p \rho_p \varepsilon_{fp}, \tag{4}$$

where k_{fp} is the covariance of fluid-particle velocity. The dissipation of particle energy in Eq. (3) is neglected because of the assumption of elastic collisions in the DNS study. The interphase TKE transfer term Π_{k_p} accounts for the influence of fluid-phase turbulence on k_p. The time scale τ_{12}^F is the particle response time.

In the equation for fluid-particle covariance k_{fp}, the interphase $\Pi_{k_{fp}}$ transfer is modeled as

$$\Pi_{k_{fp}} = -\alpha_p \rho_p \frac{1}{\tau_{12}^F} [(1 + \phi)k_{fp} - 2k_f - 2\phi k_p],$$

where $\phi = \alpha_p \rho_p / \alpha_f \rho_f$, is the mass loading. The term ε_{fp} accounts for the dissipation of k_{fp} due to viscous effects in the fluid phase and the loss of correlation by crossing–trajectory effects. This dissipation rate is modeled as $\varepsilon_{fp} = k_{fp}/\tau_{12}^t$, where τ_{12}^t is the time scale of the fluid turbulent motion viewed by the particles. The model specification for this time scale is

$$\tau_{12}^t = \tau_1^t [1 + c_\beta \xi_r^2]^{-1/2}, \quad \text{where } \xi_r = \frac{|\bar{V}_r|}{\sqrt{\frac{2}{3}k_f}},$$

where c_β varies with the angle between the mean particle velocity and the mean relative velocity. This angle is taken to be zero in the homogeneous turbulence case, resulting in $c_\beta = 0.45$. The time scale of the energetic turbulent eddies τ_1^t is

$$\tau_1^t = \frac{3}{2} C_\mu \frac{k_f}{\varepsilon_f},$$

where $C_\mu = 0.09$.

The effective particle response frequency F_D is given in terms of local mean particle Reynolds number Re_p,

$$F_D = \frac{3}{4} \frac{C_D}{d} \langle |\bar{v}_r| \rangle_2, \quad \langle |\bar{v}_r| \rangle_2 = \sqrt{V_{r,i} V_{r,i} + \langle v'_{r,i} v'_{r,i} \rangle_2}$$

$$C_D = \frac{24}{\mathrm{Re}_p}[1 + 0.15\mathrm{Re}_p^{0.687}]\alpha_f^{-1.7}, \quad \text{for } \mathrm{Re}_p < 1000,$$

where the particle Reynolds number Re_p is defined as

$$\mathrm{Re}_p = \frac{\alpha_f \langle|\bar{v}_r|\rangle_2 \bar{d}}{\nu_f}. \tag{5}$$

The averaging method $\langle\cdot\rangle_2$ is defined as the dispersed phase mass average in model I. The average value of the local relative velocity between each particle and the surrounding fluid flow $V_{r,i}$ can be expressed as

$$V_{r,i} = [U_{p,i} - U_{f,i}] - V_{d,i} \quad V_{d,i} = \langle\tilde{u}_{f,i}\rangle_2 - U_{f,i} = \langle u'_{f,i}\rangle_2, \tag{6}$$

where $U_{p,i}$ and $U_{f,i}$ are the mean velocity of each phase; the drifting velocity $V_{d,i}$ represents the correlation between the instantaneous distribution of particles and turbulent fluid motion on characteristic length scales which are large compared to the particle diameter. To apply model I in this simple test case, some quantities need to be specified. One is $\langle|v|_r\rangle_2$, the magnitude of the averaged value of the local relative velocity between particles and the surrounding fluid flow. In model I, $\langle|v_r|\rangle_2$ is defined as

$$\langle|v_r|\rangle_2 = \sqrt{V_{r,i}V_{r,i} + \langle v'_{r,i}v'_{r,i}\rangle_2},$$

where $V_{r,i}$ is the mean relative or slip velocity, which is zero in the homogeneous particle-laden decaying turbulent flow, and $v'_{r,i}$ needs to be modeled. In this study, the following approximation is used:

$$v'_{r,i} \equiv \alpha_f \alpha_p (u'_f + u'_p),$$

where $u'_f = \sqrt{2/3k_f}$, $u'_p = \sqrt{2/3k_p}$.

Also in model I, the fluid-particle velocity covariance k_{fp} needs to be initialized. If the fluid-particle velocity covariance is expressed as

$$k_{fp}(t) = \rho_{fp}(t) \cdot k_f^{1/2}(t) \cdot k_p^{1/2}(t), \tag{7}$$

then $\rho_{fp}(t)$ is a "fluid-particle" correlation coefficient, which should be bounded by 0 and 1 (based on the Cauchy-Schwarz inequality. [Implementations of this model[10] do not impose the bounds on ρ_{fp}, and recommend specification of values up to 2 so as to improve the model predictions. In this work also, $\rho_{fp}(0)=2.0$ is used.]. Using this definition, we can determine $k_{fp}(0)$ by setting $\rho_{fp}(0)$ values. The role of the quantity k_{fp}, which is really a single-point surrogate for the fluid-particle velocity covariance, is discussed in detail elsewhere.[23] It is argued that k_{fp} is not an independent flow variable in single-point closures of two-phase turbulent flows. This conclusion is consistent with the theoretical analysis presented in Sundaram and Collins [cf. Eqs. (29c) and (29d) on p. 113 in Ref. 11].

The principal time scale in the model is τ_{12}^F, the particle response time, which is related to the inertial effects acting on the particles,

$$\tau_{12}^F = F_D^{-1}\frac{\rho_p}{\rho_f}. \tag{8}$$

However, this time scale is based on the slip velocity $\langle|\bar{v}_r|\rangle_2$, which is defined on the basis of $u'_f \sim \sqrt{k_f}$ and $u'_p \sim \sqrt{k_p}$. Since

the particle Reynolds number Re_p is based on $\langle|\bar{v}|\rangle_2$, and is approximately unity in this flow, the time scale τ_{12}^F can be further simplified as

$$\tau_{12}^F = \frac{4}{3}\frac{\bar{d}}{C_D\langle\bar{v}_r\rangle_2}\frac{\rho_p}{\rho_f} = \frac{4}{3}\frac{\bar{d}}{C_D\mathrm{Re}_p\nu_f}\frac{\rho_p}{\rho_f} \approx \frac{\alpha_f\bar{d}^2}{18\nu_f}\frac{\rho_p}{\rho_f}.$$

Since $\mathrm{Re}_p \approx 1$, the product of C_D and Re_p is approximately equal to 24. Hence, in this homogeneous turbulence, under the condition of all particles having Re_p approximately equal to 1, the particle response time is approximately constant during the TKE evolution.

The prediction from model I is that TKE in the fluid phase decreases monotonically, but the net effect of particles to reduce fluid energy is found to *decrease* with increasing Stokes numbers, which is *opposite* to the DNS result (see Fig. 1). The model predictions for fluid energy evolution also show a much steeper decay at the beginning than the DNS result. The same steep decay is also observed in the particle energy evolution, which is shown in Fig. 2. The particle energy decays monotonically. The decay of particle energy is observed to increase with increasing particle Stokes numbers after $t/T_e = 0.8$, which is consistent with DNS data, but there is some crossover at the beginning of evolution, as seen in Fig. 2.

B. Model II—Ahmadi's model: Model description and results

The evolution equations of TKE in fluid and particle phase from model II,[6,7] simplified for decaying homogeneous particle-laden turbulent flow, are

$$\rho_f\alpha_f\frac{dk_f}{dt} = 2D_0(k_p - ck_f) - \rho_f\alpha_f\varepsilon_f, \tag{9}$$

$$\rho_p\alpha_p\frac{dk_p}{dt} = 2D_0(ck_f - k_p). \tag{10}$$

(In model II,[6,7] the notation used to represent fluid and particle-phase variables and volume fraction is slightly different.)

The transport equation for the dissipation rate in the fluid phase is given by Ahmadi,[24] which is essentially the same as that in the standard k-ε model for single-phase turbulence. For decaying homogeneous turbulence, the evolution equation for ε_f is

$$\alpha_f\rho_f\frac{d\varepsilon_f}{dt} = -C_{\varepsilon,2}\frac{\varepsilon_f^2}{k_f}, \tag{11}$$

where $C_{\varepsilon,2} = 1.92$. Since particle collisions are elastic in the DNS test case, the dissipation rate of particle energy is taken to be zero in model II.

The coefficient c is related to the ratio of the particle time scale $\rho_p\alpha_p/D_0$ to the macroscale Lagrangian turbulence time scale T_L,
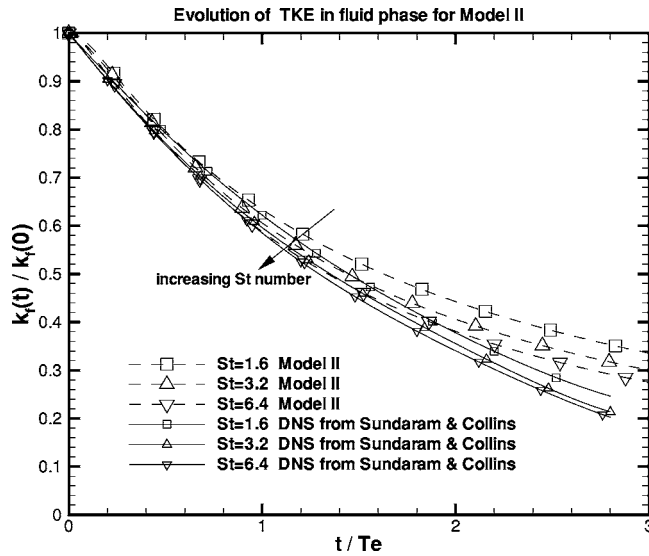
FIG. 3. Evolution of TKE in fluid phase from model II for decaying homogeneous particle-laden turbulent flow.

FIG. 4. Evolution of TKE in particle phase from model II for decaying homogeneous particle-laden turbulent flow.

$$c = \cfrac{1}{1 + \cfrac{\rho_p \alpha_p}{D_0 T_L}}, \quad T_L = \frac{0.165 k_f}{\varepsilon_f}.$$

The drag coefficient D_0 is given as

$$D_0 = \frac{18 \mu_f \alpha_p}{\bar{d}^2} \frac{[1 + 0.1(\mathrm{Re}_p)^{0.75}]}{\left(1 - \cfrac{\alpha_p}{\nu_m}\right)^{0.25 \nu_m}}, \tag{12}$$

where $\bar{d}$ is the mean particle diameter and model coefficient $\nu_m = 0.643\,56$. The particle Reynolds number Re_p is defined as

$$\mathrm{Re}_p = \frac{\rho_f \bar{d} |U_{f,i} - U_{p,i}|}{\mu_f},$$

where $U_{f,i}$ and $U_{p,i}$ are the ith components of the mean velocity in the fluid and particle phase, respectively.

In model II the term $D_0/(\alpha_p \rho_p)$ represents a particle response frequency. The expression for this particle response frequency [cf. Eq. (12)] can be further simplified because the particle Reynolds number Re_p based on the mean slip velocity is zero in this case. In the limit of volumetrically dilute flow ($\alpha_p \ll 1$), the resulting simplified expression for the particle response frequency tends to its limiting value of the reciprocal of the particle response time,

$$\frac{D_0}{\alpha_p \rho_p} = \frac{18 \nu_f}{d^2} \frac{\rho_f}{\rho_p} \frac{1}{\left(1 - \cfrac{\alpha_p}{\nu_m}\right)^{0.25 \nu_m}} \approx \frac{18 \nu_f}{d^2} \frac{\rho_f}{\rho_p} \quad \text{for } \alpha_p \ll 1.$$

Figure 3 shows that the prediction from model II shows satisfactory agreement with DNS results for the evolution of fluid energy, except for some quantitative difference after $t/T_e = 1.5$. The decay of k_f is not enough after $t/T_e = 1.5$. This is probably because the single-phase turbulence model is
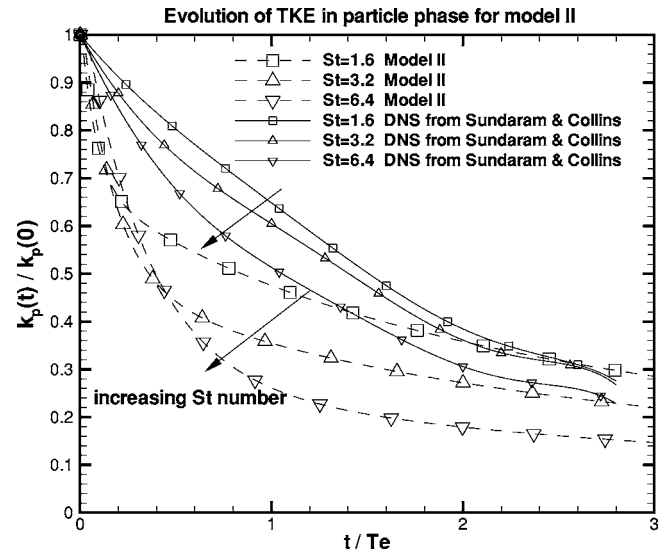
used for the dissipation rate of fluid energy. The incorrect variation of fluid energy evolution with increasing particle Stokes numbers that was observed in model I is not found in model II. Model II predicts a very steep decay of particle energy at early time, and the quantitative discrepancy between model predictions and DNS data is quite large, as seen in Fig. 4.

C. Summary of model results

It is obvious that the definition of the particle response time in model I is almost the same as that in model II under conditions of particle Reynolds number close to unity, and particle volume fraction far less than 1. The particle response time is used as the time scale for interphase TKE transfer term in both these models, and the interphase TKE transfer plays the dominant role in the equation system of both models. We arrived at this conclusion based on the budget study of the equation systems of the two multiphase turbulence models, and the detailed budget analysis is shown in Ref. 23. Given the significant discrepancy between the TKE decay rate predicted by the models and that predicted by the DNS for different Stokes numbers, it is hypothesized that the particle response time is not the appropriate time scale for interphase TKE transfer.

The physical reason behind the incorrect behavior of k_f evolution with increasing particle Stokes number in model I, and the anomalous steep decay of k_p at early time lies in the fact that the particle response time is the appropriate time scale for only a limited range of particle-eddy interactions. In reality, particle-turbulence interaction is a complex multiscale process. Even for a monodisperse gas-solid two-phase flow, particles interact with a range of eddies with different length and time scales. Furthermore, the particle response time and the Stokes number for each particle is different, since each particle has a different instantaneous velocity. The

particle response time defined here can only represent the characteristic time scale of particles interacting with the eddies in the dissipation range.

In Eulerian-Eulerian models, all the quantities in the governing equations are averaged. Since the interphase TKE transfer represents the average interaction of all particles with the entire range of turbulent scales, the model for this term should somehow account for this complex multiscale interaction.

III. MULTISCALE INTERACTION MODEL FOR INTERPHASE TKE TRANSFER

Based on the discussion in the previous section, a new time scale is proposed to model the interphase TKE transfer. This new time scale is implemented in model I and model II, and it improves the performance of both models in decaying homogeneous particle-laden turbulent flow.

From the model testing in the previous section, it was noted that the incorrect variation of k_f with increasing particle Stokes numbers, and the steep decay of k_p that are found in the model results, need to be improved. In model I and model II, the complex particle-fluid interaction represented by the interphase TKE transfer terms, is characterized by a single time scale, the particle response time τ_p, which needs further improvement. A multiscale interaction model was first proposed by Pai and Subramaniam,[25] to improve the multiphase turbulence model in KIVA,[26] which is based on the Lagrangian-Eulerian approach. An equivalent form of this multiscale interaction model is implemented in the Eulerian-Eulerian models discussed in this work, and this time scale improves the predictions from model I and model II.

One can define a particle Stokes number based on τ_l, a characteristic time scale for an eddy in the inertial subrange of turbulence, as

$$St_l = \frac{\tau_p}{\tau_l},$$

where

$$\tau_l = \frac{l}{|\mathbf{u}_g'|} = \frac{|\mathbf{u}_g'|^2}{\varepsilon_f},$$

such that l is the characteristic length scale of the eddy, and $|\mathbf{u}_g'|$ is the characteristic eddy velocity in inertial subrange. Therefore, the particle Stokes number based on τ_l scales as

$$St_l \sim \frac{1}{|\mathbf{u}_g'|^2}.$$

For the EE implementation, the distribution of $\mathbf{u}_g'$ is assumed to be joint normal for homogeneous turbulence. This means that energetic eddies can be associated with a small Stokes number and small fluctuations can be associated with a large Stokes number. Thus, there are different particle Stokes numbers St_l that correspond to eddy of different sizes l.

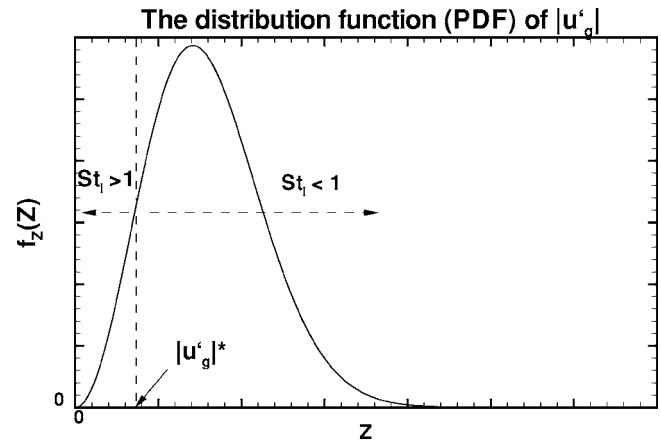The hypothesis is that for $St_l < 1$, particles respond immediately to the flow. When particles are entrained in the

FIG. 5. Sketch of the probability density function $Z = |\mathbf{u}_g'|$.

eddies with $St_l < 1$, particles will basically follow the characteristic time scale of the eddies. As St_l approaches zero, particles follow the eddy turnover time τ.

For $St_l > 1$, the particle responds slowly to the flow. In this case, the characteristic size of the eddies is small and $|\mathbf{u}_g'|^2$ is also very small. Particles will not be entrained in these small eddies. The inertia of the particle plays an important role when particle interacts with small-size eddies. Since the particle response time is a measure of the particle inertia, which depends on the density and the size of the particles, the particle follows its response time when $St_l > 1$.

For the case of zero-gravity homogeneous particle-laden turbulent flow, the fluctuating velocity in the fluid phase is assumed to be isotropic and joint normal, and the probability density function for $Z = |\mathbf{u}_g'|$ is

$$f_Z(z) = \sqrt{\frac{2}{\pi}} \frac{1}{\sigma_f^3} z^2 e^{-z^2/2\sigma_f^2},$$

where z is the corresponding sample space variable of random variable Z, and σ_f is the standard deviation of $\mathbf{u}_g'$, which is $\sqrt{2/3k_f}$ for isotropic homogeneous turbulent flows. Figure 5 is a sketch of the probability density function of Z. The value of Z, where $St_l = \tau_p/\tau_l = 1$, is of special significance and is denoted $|\mathbf{u}_g'|^*$. This transition value of $|\mathbf{u}_g'|^*$ divides the z axis into two regions: $St_l < 1$ and $St_l > 1$.

The interaction time τ_i is assumed to be a random variable, which is a prescribed function of $Z = |\mathbf{u}_g'|$. The mean interaction time $\langle \tau_i \rangle$ is obtained from the conditional mean $\langle \tau_i | Z = |\mathbf{u}_g'| \rangle$ by

$$\langle \tau_i \rangle = \int_0^\infty \langle \tau_i | z \rangle f_Z(z) dz.$$

The conditional mean of τ_i is assumed to be of the following form:

$$\langle \tau_i | Z \rangle = \tau_p, \quad 0 < |\mathbf{u}_g'| < |\mathbf{u}_g'|^*, \tag{13}$$

$$\langle \tau_i | Z \rangle = St_l \cdot (\tau_p - \tau) + \tau, \quad |\mathbf{u}_g'|^* < |\mathbf{u}_g'| < \infty. \tag{14}$$

The conditional mean $\langle \tau_i | Z \rangle$ in the range $|\mathbf{u}_g'|^* < |\mathbf{u}_g'| < \infty$ is simply modeled as a linear function of St_l. As $St_l \to 0$ $\langle \tau_i | Z \rangle$ is equal to the eddy turnover time τ and particles just move
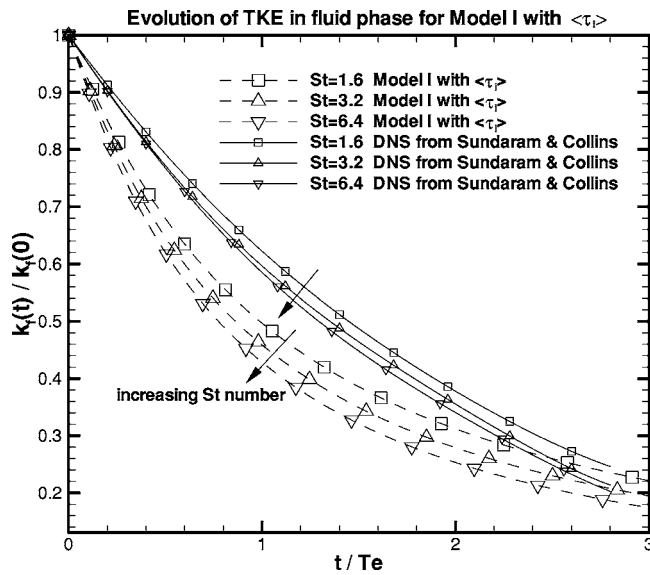
FIG. 6. Evolution of TKE in fluid phase from model I with the multiscale interaction time scale $\langle \tau_i \rangle$. Comparison of model results with DNS data.
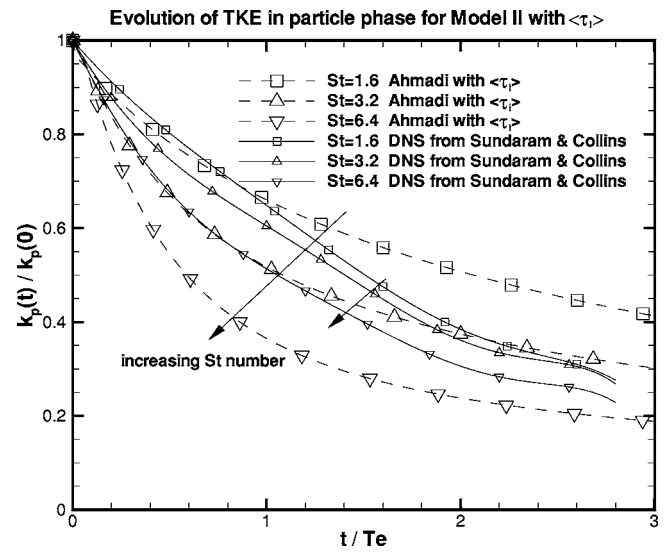

FIG. 7. Evolution of TKE in particle phase from model II with the multiscale interaction time scale $\langle \tau_i \rangle$. Comparison of model results with DNS data.

with the eddies. When $St_l \gtrsim 1$, particles respond slowly to the flow, and the particle response time τ_p is dominant here.

One can retrieve model I and model II from the expression of $\langle \tau_i \rangle$ by considering the limit of $|\mathbf{u}'_g|^* \to \infty$ and $\langle \tau_i \rangle|_{|\mathbf{u}'_g|^* \to \infty} = \tau_p$, where τ_p is the particle response time. This means that particles respond to the flow at the particle response time scale for the entire range of $|\mathbf{u}'_g|$.

The mean of τ_i is defined as

$$\langle \tau_i \rangle = \int_0^{|\mathbf{u}'_g|^*} \tau_p f_Z(z) dz + \int_{|\mathbf{u}'_g|^*}^{\infty} [St_l \cdot (\tau_p - \tau) + \tau] \cdot f_Z(z) dz,$$

(15)

where $f_Z(z)$ is the probability density function of $|\mathbf{u}'_g|$.

This new multiscale interaction time scale is implemented in both multiphase turbulence models investigated in this study. For model I, Eqs. (1)–(4) are solved with τ_{12}^F replaced by $\langle \tau_i \rangle$. With the implementation of $\langle \tau_i \rangle$ in model I, the steep decay at the beginning of k_f and k_p evolution is improved, and the incorrect trend of k_f decay with increasing particle Stokes numbers is also corrected, as seen in Fig. 6. For model II, Eqs. (9)–(11) are solved with $\alpha_p \rho_p / D_0$ replaced by $\langle \tau_i \rangle$. The fast decay of particle energy at the beginning of the evolution is eliminated after the implementation of $\langle \tau_i \rangle$ (see Fig. 7). The incorporation of the multiscale interaction time scale improves the performance of both models tested in this study.

IV. THE EQUILIBRATION OF ENERGY MODEL

Turbulence models for particle-laden flows reviewed in this study use the particle response time τ_p as the time scale for interphase TKE transfer, which results in a very steep decay of particle-phase TKE compared with DNS results. In model I, the decay of k_f with increasing particle Stokes numbers is incorrect. Model I requires an equation for the fluid-particle velocity covariance k_{fp}, which is a pseudoflow quan-

tity, and it is unclear how this quantity should be initialized and how its boundary values should be specified. Model II uses the single-phase dissipation rate model for turbulent two-phase flows. For all of these reasons, both models are deemed unsatisfactory for general applications.

A new model is proposed in this study that incorporates the mean multiscale interaction time scale, $\langle \tau_i \rangle$, and seeks to address some of the difficulties encountered in model I and model II. This model is formulated by considering the behavior of a two-phase flow system in the limit of stationary turbulence. In this limit, the mixture TKE is kept constant by artificially forcing the fluid turbulence in a homogeneous particle-laden turbulent flow. The particle-phase TKE k_p and fluid energy k_f evolve to their respective equilibrium values, k_f^e and k_p^e, over a TKE transfer time scale τ_{π}, where the superscript e denotes the quantity at the equilibrium state. At the equilibrium state, the ratio of specific fluid energy e_f^e to the specific mixture TKE e_m is a constant, which may depend on mass loading ϕ, particle Stokes number St, particle Reynolds number Re_p, and other nondimensional parameters.

In Sec. IV B, transport equations for the Reynolds stress tensor in the fluid and particle phases are derived based on the equilibration of energy concept. For simplicity of exposition, we first present the EEM model in the simple case of decaying homogeneous turbulence. The k-ε equation implied by the EEM Reynolds stress model is used to simulate the test case discussed in Sec. II.

A. Description of EEM

The model equations are written in terms of specific energy $e_f = \rho_f \alpha_f k_f$ and $e_p = \rho_p \alpha_p k_p$, which are the contributions to the total mixture energy $e_m = \rho_m k_m$ from both phases, where $\rho_m = \rho_f \alpha_f + \rho_p \alpha_p$ is the mixture density. For the decaying homogeneous turbulence, the following equation system holds:

$$\frac{de_f}{dt} = -\frac{(e_f - e_f^e)}{\tau_\pi} - \rho_f \alpha_f \varepsilon_f, \tag{16}$$

$$\frac{de_p}{dt} = -\frac{(e_p - e_p^e)}{\tau_\pi}. \tag{17}$$

For the test case considered in this study, elastic collisions are assumed in the particle phase, and there is no dissipation of particle energy. However, the dissipation of particle energy arising from inelastic collisions can be easily incorporated into Eq. (17) if necessary.

Adding Eqs. (16) and (17), the evolution equation for e_m is obtained,

$$\frac{de_m}{dt} = -\rho_f \alpha_f \varepsilon_f,$$

where the specific mixture energy e_m decays by dissipation in the fluid phase. It is assumed that the interphase TKE transfer term is conservative, in the sense that $\Pi_{k_f} = -\Pi_{k_p}$. In model II, the interphase TKE transfer terms are conservative, while the interphase TKE transfer terms in model I are not conservative.

The equilibrium values of fluid and particle-phase specific energy, $e_f^e = \rho_f \alpha_f k_f$ and $e_p^e = \rho_p \alpha_p k_p$, are determined by a model constant C_2, which is defined as

$$\frac{e_p^e}{e_m} = C_2, \quad \frac{e_f^e}{e_m} = 1 - C_2, \tag{18}$$

where C_2 must be bounded by 0 and 1. The model parameter C_2 is the fraction of the specific mixture energy present in the particle phase at equilibrium. The definition of C_2 can be rewritten as

$$C_2 = \frac{\rho_p \alpha_p k_p^e}{\rho_m k_m} = \frac{\rho_p \alpha_p k_p^e}{\rho_f \alpha_f k_f^e + \rho_p \alpha_p k_p^e} = \frac{\phi \dfrac{k_p^e}{k_f^e}}{1 + \phi \dfrac{k_p^e}{k_f^e}}. \tag{19}$$

Based on dimensional analysis, C_2 can be a function of mass loading ϕ, particle volume fraction α_p, particle Stokes number $St_\eta = \tau_p / \tau_\eta$, particle Reynolds number Re_p, and the initial k_f / k_p ratio. Recall that τ_η is the Kolmogorov time scale and τ_p is the particle response time, which is defined as

$$\tau_p = \frac{\rho_p \overline{d}^2}{\rho_f 18\nu},$$

where $\overline{d}$ is the mean particle diameter. As the particle response time τ_p increases, it takes longer for the particles to respond to the instantaneous turbulent fluctuations in the fluid phase. For two-phase turbulent flows with constant mass loading ϕ, smaller particle response time τ_p will drive the particle-phase equilibrium energy k_p^e closer to the fluid-phase equilibrium energy k_f^e. In the limit of zero Stokes number, the energy in fluid and particle phases is equal and $C_2 = \phi/(1+\phi)$. For a constant particle Stokes number, increas-

ing mass loading would increase the fraction of specific mixture energy in the particle phase at equilibrium.

A model for the fluid-phase dissipation rate is needed to close the equation system Eqs. (16) and (17). The fluid-phase dissipation rate ε_f in EEM is modeled similar to Simonin's proposal [cf. Eq. (2)] as

$$\alpha_f \rho_f \frac{d\varepsilon_f}{dt} = -C_{\varepsilon,3} \frac{\varepsilon_f (e_f - e_f^e)}{k_f \quad \tau_\pi} - C_{\varepsilon,2} \frac{\varepsilon_f^2}{k_f}, \tag{20}$$

where the first term represents the influence from interphase TKE transfer (and is modeled as $C_{\varepsilon,3} \varepsilon_f / k_f \Pi_{k_f}$), and the second term represents the dissipation of dissipation rate. Although the EEM dissipation equation is similar to Simonin's proposal, the dissipation rate predicted by EEM is different from model I. This is because the interphase TKE transfer term is modeled differently: EEM has no k_{fp} variable, and the interphase TKE transfer time scale is τ_π, whereas in model I it is proportional to the particle response time.

The concept of the equilibration of energy, and the multiscale interaction time scale $\langle \tau_i \rangle$ discussed in Sec. III, are easily extended to formulate the corresponding transport equations for the Reynolds stress in gas-solid two-phase turbulent flows.

B. Transport equation for Reynolds stress

The Reynolds stress in phase β in a two-phase flow is defined as[3,4,27,28]

$$R_{\beta,ij} \equiv \frac{\langle I_\beta \rho u'_{\beta,i} u'_{\beta,j} \rangle}{\langle I_\beta \rho \rangle}, \tag{21}$$

where $\beta = f$ denotes the fluid phase, $\beta = p$ represents the particle phase, $\langle \cdot \rangle$ denotes the ensemble average, and I_β is the indicator function for phase β. For constant thermodynamic density, $\langle I_\beta \rho \rangle$ simplifies to $\alpha_\beta \rho_\beta$, where α_β is the volume fraction and ρ_β is the density in the βth phase. The fluctuating velocity in phase β is denoted $u'_{\beta,i}$.

A general transport equation for two-phase turbulent flows is derived in Refs. 4 and 27. For gas-solid two-phase flows with the constant thermodynamic density in both phases and with no interphase mass transfer, the transport equation for the Reynolds stress in phase β simplifies to

$$\langle I_\beta \rho_\beta \rangle \left[\frac{\partial}{\partial t} + U_{\beta,k} \frac{\partial}{\partial x_k} \right] R_{\beta,ij} + \frac{\partial}{\partial x_k} \langle I_\beta \rho u'_{\beta,i} u'_{\beta,j} u'_{\beta,k} \rangle$$

$$= -\langle I_\beta \rho u'_{\beta,i} u'_{\beta,k} \rangle \frac{\partial U_{\beta,j}}{\partial x_k} - \langle I_\beta \rho u'_{\beta,j} u'_{\beta,k} \rangle \frac{\partial U_{\beta,i}}{\partial x_k}$$

$$+ \left\langle u'_{\beta,i} \frac{\partial (I_\beta \tau_{kj})}{\partial x_k} \right\rangle + \left\langle u'_{\beta,j} \frac{\partial (I_\beta \tau_{ki})}{\partial x_k} \right\rangle$$

$$+ \langle u'_{\beta,i} S_{\beta,Mj} \rangle + \langle u'_{\beta,j} S_{\beta,Mi} \rangle. \tag{22}$$

The terms on the first line from left to right are the material derivative of the Reynolds stress in phase β following $U_{\beta,k}$ (the mean velocity in phase β), the triple velocity correlation term. The terms on the second line are the production of Reynolds stress due to the mean velocity gradients. The

terms on the third line are fluctuating velocity-stress gradient correlation. The terms on the fourth line are fluctuating velocity-interfacial momentum transfer correlation. In Eq. (22), $S_{\beta,Mj}$ is the interphase momentum transfer source term in phase β. In the above equation, the production terms and the material derivative of Reynolds stress are in closed form. The triple velocity correlation term, and the fluctuating velocity-interfacial momentum transfer correlation terms need model closures.

1. Triple velocity correlation term

The triple velocity correlation term in fluid phase is modeled using the gradient-diffusion concept,

$$\frac{\partial}{\partial x_k}\langle I_f \rho u'_{f,i} u'_{f,j} u'_{f,k}\rangle = \frac{\partial}{\partial x_k}\left[\alpha_f \rho_f C_s \frac{k_f^2}{\varepsilon_f}\frac{\partial}{\partial x_k}\langle u'_{f,i}u'_{f,j}\rangle\right], \quad (23)$$

where C_s is a model constant.

In the particle-phase Reynolds stress equation, the triple velocity correlation term is also modeled using the gradient-diffusion concept as

$$\frac{\partial}{\partial x_k}\langle I_p \rho u'_{p,i} u'_{p,j} u'_{p,k}\rangle = \frac{\partial}{\partial x_k}\left[\alpha_p \rho_p C_{s,p}\langle\tau_i\rangle k_p \frac{\partial}{\partial x_k}\langle u'_{p,i}u'_{p,j}\rangle\right], \quad (24)$$

where $\langle\tau_i\rangle$ is the multiscale interaction time scale discussed in Sec. III and $C_{s,p}$ is a model constant. The model constants C_s and $C_{s,p}$ need to be determined based on experimental data or DNS results.

2. Interphase energy transfer terms

The fluctuating velocity-interfacial momentum transfer correlation terms in the last line of Eq. (22) are modeled using the equilibration of energy concept. For the fluid phase, the interphase energy transfer term is modeled as

$$\langle u'_{f,i} S_{f,Mj}\rangle + \langle u'_{f,j} S_{f,Mi}\rangle = -\alpha_f \rho_f \frac{(\langle u'_{f,i}u'_{f,j}\rangle - \delta_{ij}\frac{2}{3}k_f^e)}{\tau_\pi}, \quad (25)$$

where k_f^e is the fluid-phase TKE at the equilibrium state. For the particle phase, the interphase energy transfer term is modeled as

$$\langle u'_{p,i} S_{p,Mj}\rangle + \langle u'_{p,j} S_{p,Mi}\rangle = -\alpha_p \rho_p \frac{(\langle u'_{p,i}u'_{p,j}\rangle - \delta_{ij}\frac{2}{3}k_p^e)}{\tau_\pi}, \quad (26)$$

where k_p^e is the particle-phase TKE at the equilibrium state. Contracting indices of Eqs. (25) and (26) results in twice the interphase TKE transfer terms in Eqs. (16) and (17).

3. Model equation for dissipation rate in fluid-phase ε_f

The fluctuating velocity-stress gradient correlation terms in the fluid phase include the dissipation of fluid energy due to the viscous effects in the flow field, and are modeled by $\varepsilon_{f,ij} = \delta_{ij}\varepsilon_f$ as a consequence of local isotropy. The modeled evolution equation for ε_f is

$$\alpha_f \rho_f \frac{\partial \varepsilon_f}{\partial t} + \alpha_f \rho_f U_{f,i}\frac{\partial \varepsilon_f}{\partial x_i} = \alpha_f \rho_f \frac{\partial}{\partial x_i}\left(C_\varepsilon \frac{k_f}{\varepsilon_f}\langle u'_{f,i}u'_{f,j}\rangle \frac{\partial \varepsilon_f}{\partial x_i}\right)$$

$$- \alpha_f \rho_f C_{\varepsilon,1}\frac{\varepsilon_f}{k_f}\cdot\langle u'_{f,i}u'_{f,j}\rangle\frac{\partial U_{f,i}}{\partial x_j}$$

$$- \alpha_f \rho_f C_{\varepsilon,2}\frac{\varepsilon_f^2}{k_f}$$

$$+ \alpha_f \rho_f C_{\varepsilon,3}\frac{\varepsilon_f}{k_f}\cdot\frac{(k_f^e - k_f)}{\tau_\pi}, \quad (27)$$

where τ_π is the interphase TKE transfer time scale. The model constants are chosen to be $C_{\varepsilon,1}=1.44$, $C_{\varepsilon,2}=1.92$, $C_{\varepsilon,3}=1.2$, and $C_\varepsilon=0.15$. The model constants $C_{\varepsilon,1}$, $C_{\varepsilon,2}$, and C_ε are chosen after the dissipation model for single-phase turbulence.[29] The value of $C_{\varepsilon,3}$ is taken to be 1.2 as suggested by Simonin[8] in model I.

Since elastic collisions are assumed in particle phase in this study, the dissipation rate in particle energy k_p is zero in the particle-phase Reynolds stress transport equation. However, the dissipation of particle Reynolds stress due to inelastic collisions can be easily incorporated into the modeled evolution equation for the particle Reynolds stress tensor.

C. The k-ε equations for particle-laden turbulent flow

The k-ε equations for gas-solid two-phase turbulent flows can be obtained by contracting the indices of the transport equation for the Reynolds stress tensor. In the k-ε formulation, the fluid velocity covariance $\langle u'_{f,i}u'_{f,j}\rangle$ appearing in the production of Reynolds stress [cf. Eq. (22)] needs a closure model. It is modeled using a turbulent eddy viscosity ν_f^T as

$$\langle u'_{f,i}u'_{f,j}\rangle = -\nu_f^T\left[\frac{\partial U_{f,i}}{\partial x_j} + \frac{\partial U_{f,i}}{\partial x_j}\right] + \frac{2}{3}\delta_{ij}\left[k_f + \nu_f^T\frac{\partial U_{f,k}}{\partial x_k}\right]. \quad (28)$$

The turbulent eddy viscosity ν_f^T in fluid phase is modeled as

$$\nu_f^T = C_\mu \frac{k_f^2}{\varepsilon_f}.$$

The model constant C_μ could be a function of particle Stokes number St_η, and mass loading ϕ. Since there are no DNS data to validate the turbulent eddy viscosity hypothesis in turbulent particle-laden flows, the model constant C_μ is chosen to be 0.09, which is the value in single-phase turbulence models.

For relatively dense collision-dominated mixtures, the turbulent eddy viscosity in particle phase is modeled as $\mu_p^T = C_{\mu2}\alpha_p\rho_p\bar{d}(k_p)^{1/2}$ in Ahmadi's work,[6,7] where $C_{\mu2}$ is a function of particle volume fraction and $\bar{d}$ is the mean diameter of particle phase. For dilute mixtures, fluid turbulence is dominant and particles are transported by the fluid motion. It is suggested in Refs. 6 and 30 that the fluid length scale should be the relevant scale in μ_p^T. The multiscale interaction time

$\langle \tau_i \rangle$ is a function of k_f, which is the appropriate scale to model the dilute mixture. So, for particle phase, the particle velocity covariance tensor is modeled as

$$\langle u'_{p,i} u'_{p,j} \rangle = - \nu_p^T \left[\frac{\partial U_{p,i}}{\partial x_j} + \frac{\partial U_{p,j}}{\partial x_i} \right] + \frac{2}{3} \delta_{ij} \left[k_p + \nu_p^T \frac{\partial U_{f,k}}{\partial x_k} \right], \tag{29}$$

where

$$\nu_p^T = C_{\mu 2} k_p \langle \tau_i \rangle,$$

and $C_{\mu 2}$ is the model constant that can be obtained by comparing with experimental data or DNS results. This corresponds to specifying $\mu_p^T = C_{\mu 2} \alpha_p \rho_p \langle \tau_i \rangle k_p$. In this study $C_{\mu 2}$ is chosen to be 0.001.

Based on the transport equation for the Reynolds stress tensor, the k-ε model corresponding to the EEM Reynolds stress model for fluid and particle phase is

$$\alpha_f \rho_f \frac{\partial k_f}{\partial t} + \alpha_f \rho_f U_{f,i} \frac{\partial k_f}{\partial x_i} = \frac{\partial}{\partial x_j} \left(\alpha_f \rho_f \frac{\nu_f^T}{\sigma_{k_f}} \frac{\partial k_f}{\partial x_j} \right)$$

$$- \alpha_f \rho_f \langle u'_{f,i} u'_{f,j} \rangle \frac{\partial U_{f,i}}{\partial x_j} - \alpha_f \rho_f \varepsilon_f$$

$$- \alpha_f \rho_f \frac{[C_2 k_f - (1 - C_2) \phi k_p]}{\tau_\pi}, \tag{30}$$

$$\alpha_f \rho_f \frac{\partial \varepsilon_f}{\partial t} + \alpha_f \rho_f U_{f,i} \frac{\partial \varepsilon_f}{\partial x_i} = \frac{\partial}{\partial x_j} \left(\alpha_f \rho_f \frac{\nu_f^T}{\sigma_\varepsilon} \frac{\partial \varepsilon_f}{\partial x_j} \right)$$

$$- C_{\varepsilon,1} \alpha_f \rho_f \frac{\varepsilon_f}{k_f} \langle u'_{f,i} u'_{f,j} \rangle \frac{\partial U_{f,i}}{\partial x_j}$$

$$- C_{\varepsilon,2} \alpha_f \rho_f \frac{\varepsilon_f^2}{k_f}$$

$$- \alpha_f \rho_f C_{\varepsilon,3} \frac{\varepsilon_f}{k_f} \frac{[C_2 k_f - (1 - C_2) \phi k_p]}{\tau_\pi}, \tag{31}$$

$$\alpha_p \rho_p \frac{\partial k_p}{\partial t} + \alpha_p \rho_p U_{p,i} \frac{\partial k_p}{\partial x_i} = \frac{\partial}{\partial x_j} \left(\alpha_p \rho_p \nu_p^T \frac{\partial k_p}{\partial x_j} \right)$$

$$- \alpha_p \rho_p \langle u'_{p,i} u'_{p,j} \rangle \frac{\partial U_{p,i}}{\partial x_j}$$

$$- \alpha_p \rho_p \frac{\left[(1 - C_2) k_p - \frac{C_2}{\phi} k_f \right]}{\tau_\pi}, \tag{32}$$

where $\sigma_{k_f} = 1.0$ and $\sigma_\varepsilon = 1.3$.

TABLE I. The coefficients for EEM.

C_μ	$C_{\varepsilon,2}$	$C_{\varepsilon,1}$	σ_{k_f}	σ_ε	$C_{\varepsilon,3}$	$C_{\mu 2}$	C_π
0.09	1.92	1.44	1.0	1.3	1.2	0.001	2.5

D. Model results for decaying homogeneous turbulence

In this section the simplified equations for decaying homogeneous turbulence are described. The predictions from EEM for decaying homogeneous particle-laden turbulent flows are compared with DNS results.

The EEM equation system for decaying homogeneous turbulence is

$$\frac{dk_f}{dt} = - \frac{1}{\tau_\pi} [C_2 k_f - (1 - C_2) \phi k_p] - \varepsilon_f, \tag{33}$$

$$\frac{d\varepsilon_f}{dt} = - C_{\varepsilon,3} \frac{\varepsilon_f}{k_f} \frac{[C_2 k_f - (1 - C_2) \phi k_p]}{\tau_\pi} - C_{\varepsilon,2} \frac{\varepsilon_f^2}{k_f}, \tag{34}$$

$$\frac{dk_p}{dt} = - \frac{1}{\tau_\pi} \left[(1 - C_2) k_p - \frac{C_2}{\phi} k_f \right]. \tag{35}$$

The interphase TKE transfer time scale τ_π is related to the multiscale interaction time scale $\langle \tau_i \rangle$ (which was introduced in Sec. III) by the expression

$$\tau_\pi = \frac{\langle \tau_i \rangle}{C_\pi} \quad \text{or} \quad C_\pi = \frac{\langle \tau_i \rangle}{\tau_\pi}, \tag{36}$$

where C_π is chosen to be 2.5 in this model.

As discussed in Sec. IV A, in general C_2 is a function of mass loading ϕ, particle volume fraction α_p, particle Stokes number St_η, particle Reynolds number Re_p, and initial k_f/k_p ratio. In the absence of relevant data from DNS of stationary turbulence, it is hypothesized that the mass loading ϕ of the system strongly affects C_2, whereas it is likely that C_2 depends very little on particle Stokes number St_η. The dependence on the particle volume fraction α_p is neglected for dilute flows. For particle Reynolds number in the Stokes regime, $Re_p \sim 1$, the dependence of C_2 on the particle Reynolds number Re_p is also neglected. For simplicity, C_2 is also assumed to be independent of initial k_f/k_p ratio, but this assumption may not be justified for initial k_f/k_p ratio far from 1. Under these assumptions, C_2 is modeled as a linear function of mass loading ϕ,

$$C_2 = 0.6\phi. \tag{37}$$

This specification is chosen such that the model predictions from EEM match well with DNS results. It is natural to require the model for C_2 to reproduce the correct limiting value $\phi/(1+\phi)$ as $St_\eta \to 0$. With the current specification of $C_2 = 0.6\phi$, the value of C_2 in the limit $St_\eta \to 0$ differs from $\phi/(1+\phi)$ by approximately 10%. The model constants used in EEM are listed in Table I.

The predictions from EEM are shown in Figs. 8 and 9. The model results match the DNS results for fluid-phase TKE evolution quite well at early time (see Fig. 8), but a
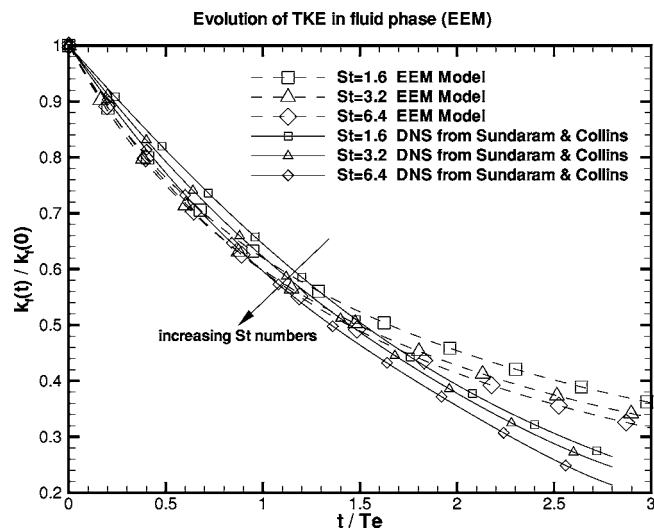
FIG. 8. Evolution of TKE in fluid phase for EEM compared with DNS data.

FIG. 10. Schematic of the flow configuration in the particle-laden homogeneous shear flow.

small quantitative discrepancy is observed after $t/T_e > 1.5$. The decay rate in particle energy shows larger separation with increasing particle Stokes number than the DNS (see Fig. 9), but the overall trend is satisfactory.

V. PARTICLE-LADEN TURBULENT HOMOGENEOUS SHEAR FLOW

In this section the test case of particle-laden homogeneous shear flow is described, and major results from the DNS study by Elghobashi[12] are discussed. The predictions from model I and EEM are then compared with DNS data.

A. Description of test case

In the DNS study of particle-laden homogeneous shear flow by Elghobashi,[12] the flow field has an identical imposed mean velocity for both phases. In the fluid phase, the x_1 component of mean velocity U varies linearly in x_3 ($U = Sx_3$), where S is the mean velocity gradient taken to be S
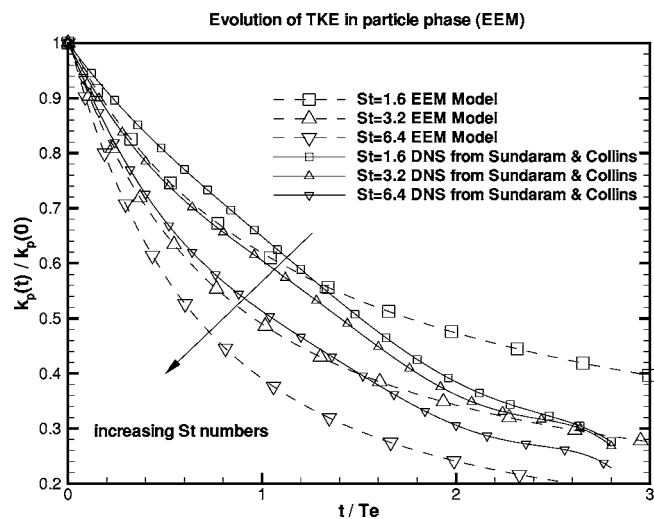
=1 in the simulation. The x_1 component of particle-phase mean velocity is also imposed with unit mean velocity gradient. The mean velocity in x_2 and x_3 direction is zero in both fluid and particle phase. A schematic of the flow configuration is shown in Fig. 10. The solid particles are rigid spheres (ρ_p is constant), and there is no interphase mass transfer. The particle volume fraction is small ($\alpha_p < 10^{-3}$), and the effect of the presence of particles on the fluid mass conservation equation is neglected. The particle size is in the sub-Kolmogorov range. The point-particle approximation is also used in this DNS study, so a linear drag law is assumed for each particle.

The major results from the particle-laden homogeneous shear flow DNS are the following:

(i)   The evolution of the fluid velocity covariance $\langle u'_{f,1} u'_{f,3} \rangle$ is reported for $\tau_p = 1.0$ and mass loading $\phi = 1.0$. The fluid velocity covariance is important to validate the assumption of turbulent eddy viscosity in Eq. (28).

(ii) The effect of varying the particle inertia ($\tau_p = 0.1, 0.25, 0.5, 1.0$) on the evolution of fluid-phase TKE is studied. It is found that as the particle inertia increases, the decay rate of fluid-phase TKE increases (for fixed mass loading ϕ).

B. Comparative assessment of model results

The simplified governing equations for particle-laden homogeneous shear flow from model I are given in Appendix A. Model II results are not presented for the homogeneous shear test case because the volume fraction of particles in this test is well beyond the realm of applicability of model II's closure for the TKE production in particle phase (see Appendix B). The particle-phase TKE production term in model II is modeled using a turbulent eddy viscosity analogy, and is intended for rapid granular flows where the effect of the fluid phase is negligible (or secondary), and the transport of momentum is dominated by particle-particle collisions. The particle TKE production term in the k_p equation has a $1/\alpha_p$ dependence (arising from the model constant $C_{\mu2}$) that

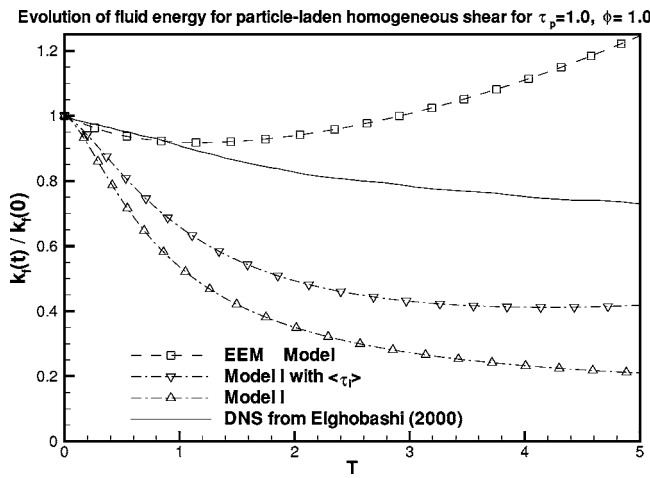FIG. 9. Evolution of TKE in particle phase for EEM compared with DNS data.

FIG. 11. Evolution of TKE in fluid phase for model I, model I with multi-scale interaction time scale $\langle \tau_i \rangle$, and EEM model for homogeneous particle-laden shear flow.

FIG. 12. Budget plot for fluid-phase TKE equation from model I for $\phi = 1.0$ and $\tau_p = 1.0$ in homogeneous particle-laden shear flow. Note that the production term equals $-\langle u'_{f,1} u'_{f,3} \rangle$ since the mean velocity gradient S is 1.

becomes unbounded in the limit $\alpha_p \to 0$. (These details of model II are given in Appendix B.) If this closure model is used for volumetrically dilute flows (the particle-laden homogeneous shear flow studied here is quite dilute, with α_p around 10^{-4}), then the particle TKE production term results in an unphysical growth of k_p. Therefore, only predictions from model I and EEM are compared with DNS results for this case.

For EEM, the simplified governing equations for homogeneous shear flow are

$$\frac{dk_f}{dt} = \Pi_{k_f} - \varepsilon_f - \langle u'_{f,1} u'_{f,3} \rangle \frac{\partial U_{f,1}}{\partial x_3}, \tag{38}$$

$$\frac{d\varepsilon_f}{dt} = \Pi_{\varepsilon_f} - \frac{\varepsilon_f}{k_f} \left[C_{\varepsilon,1} \langle u'_{f,1} u'_{f,3} \rangle \frac{\partial U_{f,1}}{\partial x_3} + C_{\varepsilon,2} \varepsilon_f \right], \tag{39}$$

$$\frac{dk_p}{dt} = \Pi_{k_p} - \langle u'_{p,1} u'_{p,3} \rangle \frac{\partial U_{p,1}}{\partial x_3}, \tag{40}$$

where Π_{k_f}, Π_{ε_f}, and Π_{k_p} represent the influence of interphase TKE transfer. The velocity covariance in the fluid phase $\langle u'_{f,i} u'_{f,j} \rangle$ and the velocity covariance in particle phase $\langle u'_{p,i} u'_{p,j} \rangle$ are modeled using the turbulent eddy viscosity concept [cf. Eqs. (28) and (29)].

For $\tau_p = 1.0$ and $\phi = 1.0$, the evolution of fluid-phase energy is compared in Fig. 11. It is found that the decay rate of k_f from model I is much steeper than DNS results, which is up to 70% off at $T = 3$. With the implementation of $\langle \tau_i \rangle$ in model I by replacing the time scale τ_{12}^F in Eqs. (1)–(4), the steep decay of fluid-phase TKE is improved, and the quantitative difference is around 30% at $T = 3$. EEM predicts the decay rate of k_f quite close to the DNS results at the beginning of evolution $T < 1$. After $T > 1$, the fluid energy starts to increase. In EEM's results, the relative error is 20% off at $T = 3$ compared with DNS results.

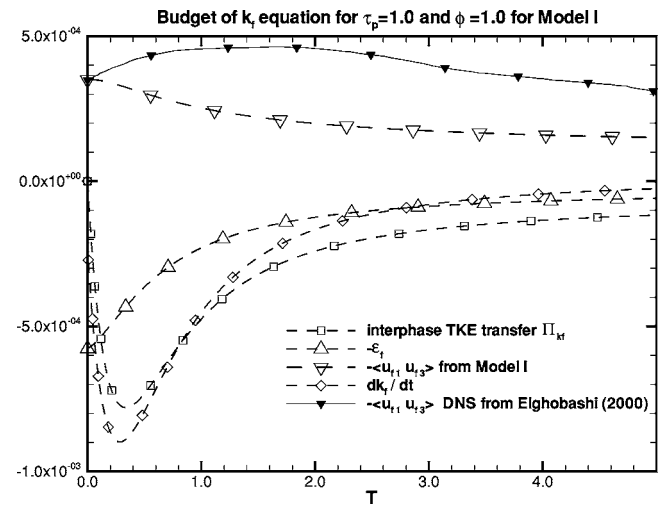For model I, the budget plot is shown in Fig. 12, which shows that the interphase TKE transfer term is dominant and

contributes most to the fast decay at early time. The budget of the interphase TKE transfer term, dissipation rate, and the production in Eq. (38) for EEM is plotted in Fig. 13. It shows that the growth of fluid-phase TKE is mainly due to the almost linear increase in the production as time evolves. The budget plot in Fig. 13 also shows that production and dissipation rate are the two major terms in the fluid energy evolution equation (interphase TKE transfer is very small). The evolution of fluid-phase dissipation rate ε_f is also reported in the DNS study. If the fluid-phase dissipation rate in the EEM model is specified from DNS data, the growth of fluid energy is eliminated, as seen in Fig. 14. This shows that if the fluid dissipation can be modeled with more accuracy, the predictions from EEM can be further improved.

The velocity covariance $\langle u'_{f,1} u'_{f,3} \rangle$ is reported for $\tau_p = 1.0$, $\phi = 1.0$ in the DNS results. Since this term determines the production term in the k-ε equations for fluid phase [cf. Eqs.
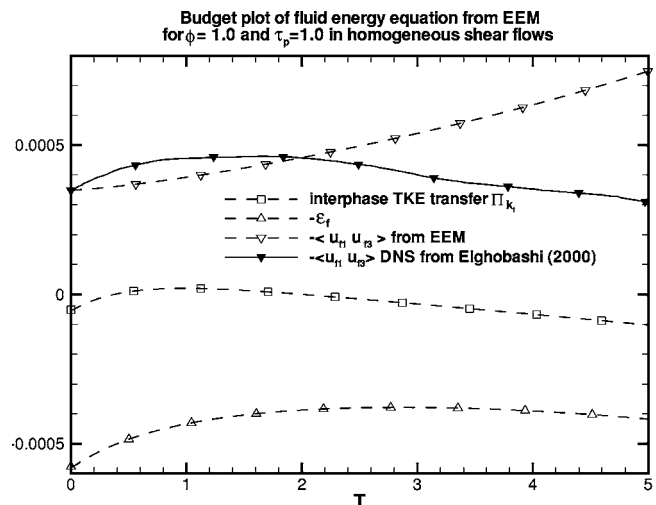

FIG. 13. Budget plot for fluid TKE equation in EEM model for $\phi = 1.0$ and $\tau_p = 1.0$ in homogeneous particle-laden shear flow. Note that the production term equals $-\langle u'_{f,1} u'_{f,3} \rangle$ since the mean velocity gradient S is 1.
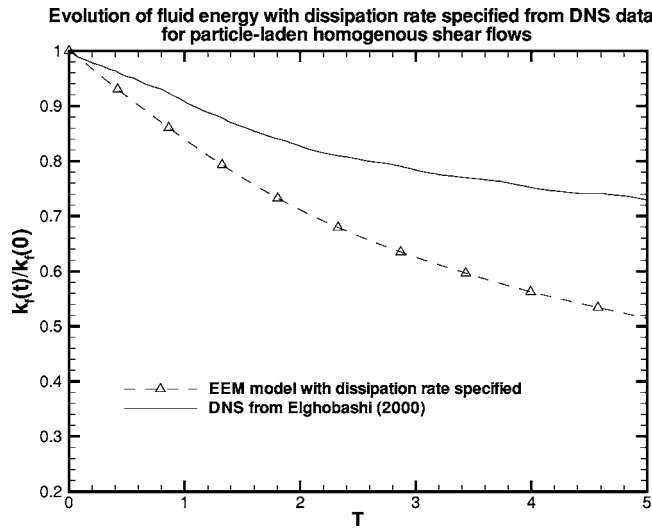
FIG. 14. Evolution of TKE in fluid phase for EEM model with dissipation rate specified from DNS results for the particle-laden homogeneous shear flow with $\phi=1.0$ and $\tau_p=1.0$. Fluid-phase TKE evolution from DNS is also shown for comparison.

FIG. 16. Evolution of TKE in fluid phase with increasing particle inertia (constant mass loading) for particle-laden homogeneous shear flow. Solid line represents DNS results; dashed line represents the predictions from model I; dash-dot line represents the results from model I improved with multiscale interaction time scale $\langle \tau_i \rangle$. The symbol $\square$ represents $\tau_p=0.1$; $\triangle$ represents $\tau_p=0.25$; $\triangledown$ represents $\tau_p=0.5$; and $\diamond$ represents $\tau_p=1.0$.

(30) and (31)], it is important to model this quantity accurately. In this test case, the velocity covariance $-\langle u'_{f,1} u'_{f,3} \rangle$ equals the shear production since the mean velocity gradient S is 1. In Figs. 12 and 13 the comparison of $\langle u'_{f,1} u'_{f,3} \rangle$ shows a large discrepancy between the DNS and model results. However, it is perhaps more appropriate to compare the correlation coefficient ρ_{f13}, which is defined as

$$\rho_{f13} = \frac{\langle u'_{f,1} u'_{f,3} \rangle}{\sqrt{\langle u'_{f,1} u'_{f,1} \rangle \langle u'_{f,3} u'_{f,3} \rangle}}, \qquad (41)$$

and this comparison is shown in Fig. 15. There is a large difference at early time, but after $T=4$ the difference is small. The discrepancy could be due to the influence of initial conditions or the interphase TKE transfer term.

The particle inertia study is performed for $\tau_p = 0.1, 0.25, 0.5, 1.0$ with the same mass loading $\phi=0.1$. DNS data show that, with the increasing particle response time, the decay rate of k_f increases. The predictions of model I are shown in Fig. 16, where model I gives the *opposite* trend with increasing particle response time τ_p (or particle inertia). After implementing the multiscale interaction time scale $\langle \tau_i \rangle$ in place of τ_{12}^F in model I, the incorrect trend of fluid-phase TKE decay rate is corrected and the evolution of fluid energy becomes closer to the DNS results, as seen in Fig. 16.

The model results from EEM for particle inertia study are shown in Fig. 17. These results are very close to DNS data, and the trend of TKE evolution with increasing particle inertia is correct. However, the difference in the decay rate of
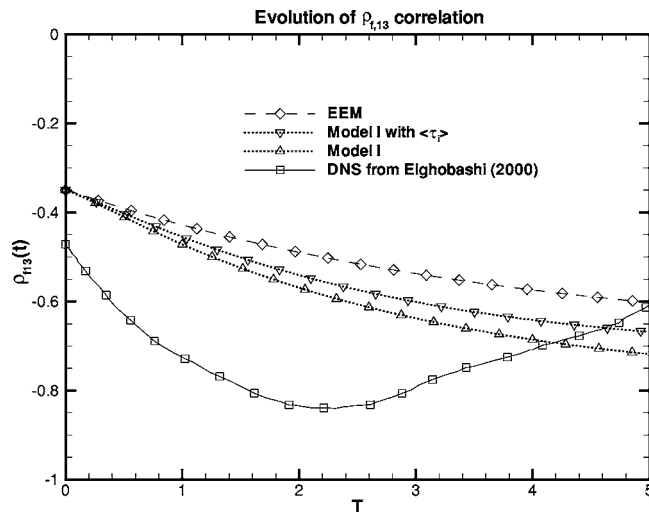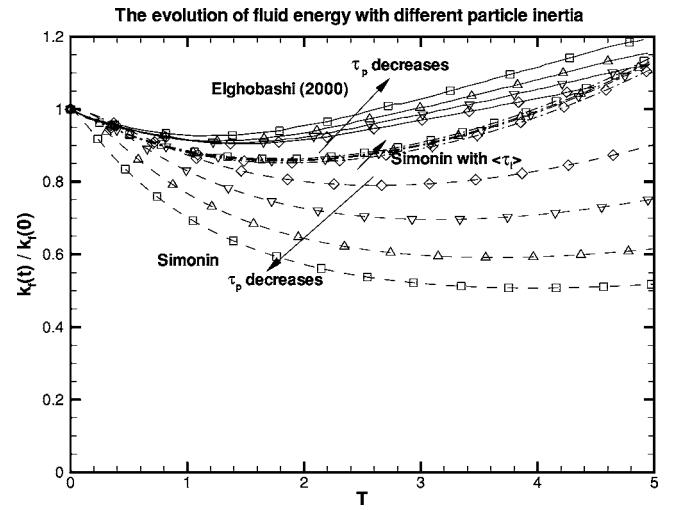

FIG. 15. Evolution of the velocity correlation ρ_{f13} for model I, model I implemented with multiscale interaction time scale $\langle \tau_i \rangle$, and EEM model in homogeneous particle-laden shear flow. DNS result is shown for comparison.
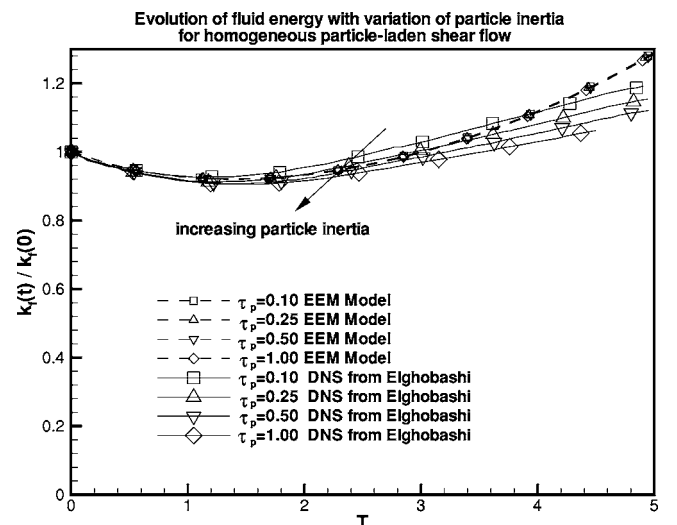

FIG. 17. Evolution of TKE in fluid phase for increasing particle response time τ_p (constant mass loading $\phi=0.1$) from EEM. DNS data are shown for comparison.

fluid energy with increasing particle inertia is too small. A possible reason for this deficiency is that there is no information of particle inertia in the fluid-phase production term. One improvement is to use $\langle \tau_i \rangle$ to substitute eddy turnover time in ν_f^T. However, without detailed DNS data for variation of shear production with different particle inertia, the model for fluid and particle shear production terms in EEM cannot be validated.

VI. DISCUSSION

With the equilibration of energy concept, the evolution of TKE in fluid and particle phase is shown to be improved when compared with the DNS results of decaying homogeneous particle-laden turbulence and homogeneous particle-laden shear flow. Incorporation of the multiscale interaction time scale $\langle \tau_i \rangle$ into model I and model II corrects the incorrect trend of k_f decay rate with increasing particle inertia, and the evolution of TKE in fluid and particle phase is shown to match with DNS results satisfactorily. Implicit in the above statement is the assumption that the DNS is itself an accurate representation of the physics of the particle-laden turbulent flows. The point-particle assumption for the *particle drag* in such DNS studies is justified in a limited flow regime where particle Reynolds numbers Re_p are of order 1, the density ratio $\rho_p/\rho_f \sim \mathcal{O}(1000)$, and particles are sub-Kolmogorov size with negligible wake effects. Also, volume displacement effects are neglected in such DNS studies, and the fluid velocity field is assumed to be solenoidal.

The homogeneous problem that forms the basis of this study, and for which the DNS database exists, corresponds to a flow regime where the aforementioned assumptions are valid. However, a good approximation to the particle drag in the DNS does not necessarily guarantee accurate calculation of the fluid-phase dissipation rate in the presence of particles. Also, particle-particle interaction effects are not accounted for in the point-particle approximation, and the effect of the point-particle approximation on the pressure field is not quantified either.

The only way to test these approximations is by performing *true* DNS, where flow field around each particle is fully resolved and exact boundary conditions are imposed on particle surface. Using such true DNS calculations, the consequence of the point-particle approximation on the solenoidality of the fluid velocity field (which will in turn affect the fluid pressure field), and the neglect of particle-particle interaction effects can be evaluated. Recent studies by Moses and Edwards[31] seek to assess the consequences of the point-particle approximation. However, their study is in 2D for considerably large cylinders (particle Reynolds number based on diameter of cylinder $Re_p=26$), with an emphasis on evaluating the effects of filtering the velocity field. Their study is relevant to the examination of the validity of LES based on the point-particle approximation. Similar studies are necessary for DNS, but such calculations are still limited by computational cost. Therefore, the DNS datasets performed with point-particle approximation that are used in this study are the best data available for model testing and validation.

It appears likely that the existing DNS database *does* capture the major trends of the TKE variation with important nondimensional parameters like Stokes numbers and mass loading. It is possible that the true DNS might revise the exact quantitative predictions. Since the principal conclusions in this study concern qualitative trends rather than an exact quantitative match between model predictions and DNS results, it is reasonable to assert that incorporation of the new multiscale interaction time scale leads to a better representation of the problem physics.

It is worthwhile to examine whether any experimental data can be used for model validation. Experimental study of nearly isotropic particle-laden turbulence includes work by Rogers.[32] This work reports the preferential concentration of particles in microgravity conditions with variation of particle Stokes number, but the turbulence kinetic energy in either phase that is required for model validation is not reported. While this experimental result is useful for models that predict preferential concentration, information of the second moments of fluid and particle fluctuating velocity that is useful for model validation is not reported.

Experimental investigation of homogeneous dilute particle-laden flows includes studies by Faeth.[33] This work investigates the settling of uniform flux of monodisperse spherical particles in a stagnant water bath. This study reports the second moments of fluctuating velocity in fluid phase varying with particle volume fraction and particle sizes, but there is no systematic study of TKE evolution with variation of important nondimensional parameters, such as particle Stokes number. The results of these experiments will be useful for further evaluation of model performance, now that the model constants have been determined based on comparison with DNS of particle-laden turbulence.

VII. SUMMARY

Two multiphase turbulence models (model I by Simonin[8,9] and model II by Ahmadi[6,7,24]) are compared with direct numerical simulations (DNS) of two canonical flows: decaying homogeneous particle-laden turbulence,[11] and homogeneous particle-laden shear flow.[12] The principal findings from this comparative assessment of the two models are the following:

(1) For homogeneous particle-laden turbulent flow, both models predict a faster decay rate of fluctuating energy (in both phases) than found in the DNS. The reason for the faster decay is that the particle response time ($\tau_p = d^2\rho_p/18\mu_f$) is used as the time scale for interphase TKE transfer in both models. For monodisperse particles there is a single particle response time scale. The results indicate that a single particle response time does not adequately characterize the interaction between the particles and the range of turbulent eddy sizes, which is responsible for interphase TKE transfer.

(2) Anomalous variation of TKE with different particle Stokes numbers is found in the model I results. The interphase TKE transfer is the dominant term in model I that causes this anomalous model behavior. A pseudoflow quantity k_{fp} is introduced in the interphase TKE

transfer terms in model I, and the particle response time is used as the relevant time scale for interphase TKE transfer.

The following areas for model improvement are identified: (i) model for interphase TKE transfer, especially the time scale of interphase TKE transfer, and (ii) correct prediction of TKE evolution with variation of particle Stokes number. In model I the fluid-particle covariance k_{fp} is introduced, which is not an independent flow variable in single-point closure of two-phase turbulent flows, and it is unclear how the initial and boundary conditions for this term should be specified. These deficiencies in model I and model II limit the application of these two models.

A new multiphase turbulence model, equilibration of energy model (EEM), is proposed in this paper. A noteworthy feature of EEM is that a multiscale interaction time scale $\langle \tau_i \rangle$ is proposed to account for the interaction of a particle with a range of eddy sizes. As the particle Stokes number approaches zero, $\langle \tau_i \rangle$ approaches the eddy turnover time; and $\langle \tau_i \rangle$ approaches particle response time τ_p in the limit of St $\rightarrow \infty$.

This new multiscale interaction time scale $\langle \tau_i \rangle$ is incorporated into the interphase TKE transfer terms of models I and II. It is found that for particle-laden isotropic turbulence, the predicted steep decay of TKE at the beginning of simulation is improved. The incorrect variation of TKE decay with increasing particle Stokes numbers in model I is also eliminated by using the time scale $\langle \tau_i \rangle$. The predictions from EEM shows satisfactory agreement with the DNS results for particle-laden isotropic turbulence.

For more complicated flow cases like the homogeneous particle-laden shear flow, the model predictions can be further improved if the dissipation rate in fluid phase is modeled with more accuracy. A difficulty that is encountered in shear flows is that the detailed budget of terms in the TKE equation is not available from existing DNS studies.

EEM is a simple model, but it has a clear physical interpretation, and it gives reasonable trends with the important nondimensional parameters of particle-laden turbulent flow such as particle Stokes number. Although many fundamental issues need to be addressed for this class of two-phase turbulence models—including realizability[34] and the assumption of local isotropy of small-scale motions—the EEM model can still be a useful engineering tool for CFD simulation of particle-laden turbulent flows.

APPENDIX A: MODEL I—MODEL EQUATION FOR HOMOGENEOUS SHEAR FLOWS

In this section, the governing equations from model I for homogeneous shear flows are described in detail.

The simplified model equations for TKE in fluid phase from model I are

$$\frac{dk_f}{dt} = -\langle u'_{f,1} u'_{f,3} \rangle \frac{\partial U_{f,1}}{\partial x_3} + \frac{\Pi_{k_f}}{\alpha_f \rho_f} - \varepsilon_f, \tag{A1}$$

$$\frac{d\varepsilon_f}{dt} = -\frac{\varepsilon_f}{k_f} C_{\varepsilon,1} \langle u'_{f,1} u'_{f,3} \rangle \frac{\partial U_{f,1}}{\partial x_3} + \frac{\Pi_{\varepsilon_f}}{\alpha_f \rho_f} - C_{\varepsilon,2} \frac{\varepsilon_f^2}{k_f}. \tag{A2}$$

The interphase TKE transfer term and dissipation term were already discussed. The production due to the mean velocity gradient takes effect in this case, and the velocity covariance $\langle u'_{f,i} u'_{f,j} \rangle$ is modeled using the turbulent eddy viscosity concept,

$$\langle u'_{f,i} u'_{f,j} \rangle = -\nu_f^T \left[\frac{\partial U_{f,i}}{\partial x_j} + \frac{\partial U_{f,j}}{\partial x_i} \right] + \frac{2}{3} \delta_{ij} \left[k_f + \nu_f^T \frac{\partial U_{f,m}}{\partial x_m} \right], \tag{A3}$$

where the turbulent eddy viscosity in fluid phase is modeled as

$$\nu_f^T = \frac{2}{3} k_f \tau_1^t = C_\mu \frac{k_f^2}{\varepsilon_f}. \tag{A4}$$

The simplified equations for TKE in particle phase are

$$\frac{dk_p}{dt} = -\langle u'_{p,1} u'_{p,3} \rangle \frac{\partial U_{p,1}}{\partial x_3} + \frac{\Pi_{k_p}}{\alpha_p \rho_p}, \tag{A5}$$

$$\frac{dk_{fp}}{dt} = -\langle u'_{f,1} u'_{p,3} \rangle \frac{\partial U_{p,1}}{\partial x_3} - \langle u'_{f,3} u'_{p,1} \rangle \frac{\partial U_{f,1}}{\partial x_3} + \frac{\Pi_{k_{fp}}}{\alpha_f \rho_p} - \varepsilon_{fp}. \tag{A6}$$

The velocity covariance tensor in particle phase is modeled with the concept of turbulent eddy viscosity,

$$\langle u'_{p,i} u'_{p,j} \rangle = -\nu_p^T \left[\frac{\partial U_{p,i}}{\partial x_j} + \frac{\partial U_{p,j}}{\partial x_i} \right] + \frac{2}{3} \delta_{ij} \left[k_p + \nu_p^T \frac{\partial U_{p,m}}{\partial x_m} \right]. \tag{A7}$$

The algebraic expression for the turbulent eddy viscosity in particle phase is obtained from the off-diagonal correlation equations written in a quasiequilibrium homogeneous shear flow, providing that the difference between the fluid and the particle mean velocity gradients remains negligible,

$$\nu_p^T = \left[\nu_{fp}^T + \frac{1}{2} \tau_{12}^F \frac{2}{3} k_p \right] \left[1 + \frac{\tau_{12}^F}{2} \frac{\sigma_c}{\tau_2^c} \right]^{-1}, \tag{A8}$$

where τ_2^c is the interparticle collision time; σ_c takes the general form

$$\sigma_c = [1 + e_c][3 - e_c]/5. \tag{A9}$$

Since the interparticle collision is assumed to be elastic ($e_c = 1$) in the DNS case, σ_c leads to the Grad's value $\sigma_c = 0.45$. Following Simonin,[35] if τ_2^c is small compared to the other time scales, the particle fluctuating motion is controlled by collisions between particles without effects from the fluid motions. On the other hand, if τ_2^c is large, the gas is expected to play a dominant role in the fluid fluctuating motion of particles. So, for very dilute gas-solid two-phase flows, τ_2^c is expected to be very large ($\tau_2^c \to \infty$). The turbulent eddy viscosity in particle phase for the dilute mixtures is further simplified as

$$\nu_p^T = \nu_{fp}^T + \frac{1}{2}\tau_{12}^F \frac{2}{3}k_p. \tag{A10}$$

The fluid-particle turbulent viscosity ν_{fp}^T is written in terms of the fluid-particle velocity covariance k_{fp} and an eddy-particle interaction time τ_{12}^t,

$$\nu_{fp}^T = \frac{1}{3}k_{fp}\tau_{12}^t. \tag{A11}$$

The fluid-particle covariance is modeled as

$$\langle u_{f,i}' u_{p,j}' \rangle = \frac{1}{3}k_{fp}\delta_{ij} + \frac{\eta_f}{1 + \eta_r}\left[\langle u_{f,i}' u_{f,j}'\rangle - \frac{2}{3}k_f\delta_{ij}\right]$$
$$- \frac{\nu_{fp}^T}{1 + \eta_r}\left[\frac{\partial U_{f,i}}{\partial x_j} + \frac{\partial U_{p,j}}{\partial x_i} - \frac{1}{3}\frac{\partial U_{f,m}}{\partial x_m}\delta_{ij}\right.$$
$$\left. - \frac{1}{3}\frac{\partial U_{p,m}}{\partial x_m}\delta_{ij}\right], \tag{A12}$$

where $\eta_r = \tau_{12}^t / \tau_{12}^F$. The closure assumption is that as particle response time tends toward 0, the fluid-particle covariance is consistent with the fluid velocity correlation.

APPENDIX B: MODEL II—MODEL EQUATION FOR HOMOGENEOUS SHEAR FLOWS

In this section, the governing equations from model II for homogeneous shear flows are described:

$$\alpha_f \rho_f \frac{dk_f}{dt} = \mu_f^T \frac{\partial U_{f,1}}{\partial x_3}\frac{\partial U_{f,1}}{\partial x_3} + 2D_0(ck_f - k_p), \tag{B1}$$

$$\alpha_f \rho_f \frac{d\varepsilon_f}{dt} = C_{\varepsilon,1}\mu_f^T \frac{\varepsilon_f}{k_f}\frac{\partial U_{f,1}}{\partial x_3}\frac{\partial U_{f,1}}{\partial x_3} - \alpha_f\rho_f C_{\varepsilon,2}\frac{\varepsilon_f^2}{k_f}, \tag{B2}$$

$$\alpha_p \rho_p \frac{dk_p}{dt} = \mu_p^T \frac{\partial U_{p,1}}{\partial x_3}\frac{\partial U_{p,1}}{\partial x_3} + 2D_0(ck_f - k_p). \tag{B3}$$

The coefficient c and drag coefficient D_0 were discussed previously. The production due to the mean velocity gradient takes effect in this case, which is modeled using the turbulent eddy viscosity concept. The turbulent eddy viscosity in fluid phase is modeled[6,7] as

$$\mu_f^T = C_\mu \alpha_f \rho_f \frac{k_f^2}{\varepsilon_f}, \tag{B4}$$

and turbulent eddy viscosity in particle phase is modeled as

$$\mu_p^T = C_{\mu 2}\alpha_p \rho_p \bar{d}k_p^{1/2}, \tag{B5}$$

where

$$C_\mu = 0.09, \quad C_{\mu 2} = 0.0853[(\chi\alpha_p)^{-1} + 3.2 + 12.1824\chi\alpha_p]. \tag{B6}$$

The crowding effect exhibits itself through the radial distribution function χ. For spherical particles and rapid granular flows, the radial distribution function χ is modeled as

$$\chi = \frac{1 + 2.5\alpha_p + 4.5904\alpha_p^2 + 4.515\,439\alpha_p^3}{\left[1 - \left(\dfrac{\alpha_p}{\nu_m}\right)^3\right]^{0.678\,021}}, \tag{B7}$$

with $\nu_m = 0.643\,56$.

In Ahmadi,[36] the value of coefficient C_μ is modified as

$$C_\mu = 0.09C_\mu^*,$$

where the coefficient C_μ^* is introduced to account for the effect of higher particle volume fraction of damping the fluid turbulence, and is given as

$$C_\mu^* = \frac{1}{1 + \dfrac{\alpha_p\rho_p}{D_0 T_L}\left(\dfrac{\alpha_p}{\nu_m}\right)^3}.$$

The drag coefficient D_0, time scale T_L, and ν_m are described in Sec. II B.

Turbulent eddy viscosity in particle phase is also modified as

$$\mu_p^T = C_{\mu 2}^* C_{\mu 2}\alpha_p \rho_p \bar{d}k_p^{1/2}, \tag{B8}$$

where $C_{\mu 2}^*$ is given as

$$C_{\mu 2}^* = \frac{1}{1 + \dfrac{T_L D_0}{\alpha_p\rho_p}\left(\dfrac{\alpha_p}{\nu_m}\right)^3}.$$

The coefficient $C_{\mu 2}^*$ is introduced in the turbulent eddy viscosity in particle phase μ_p^T to account for the reduction of collisional effect as particle response time becomes small.

[1] J. B. Eduardo, J. A. Yasuna, and J. L. Sinclair, "Dilute turbulent gas-solid flow in risers with particle-particle interactions," AIChE J. **41**, 1375 (1995).
[2] S. Dasgupta, S. Sundaresan, and R. Jackson, "Turbulent gas-particle flows in vertical risers," AIChE J. **40**, 215 (1994).
[3] D. Drew, "Mathematical modeling of two-phase flow," Annu. Rev. Fluid Mech. **15**, 261 (1983).
[4] S. Subramaniam, "Modeling turbulent two-phase flows," in 16th Annual Conference on Liquid Atomization and Spray Systems, ILASS (2003).
[5] S. Subramaniam, "Properly constrained interphase momentum transfer models for constant-density two-phase flow: Resolution of the ill-posedness issue in canonical problems," in 15th Annual Conference on Liquid Atomization and Spray Systems (2002).
[6] G. Ahmadi and D. Ma, "A thermodynamical formulation for dispersed multiphase turbulent flows. I. Basic theory," Int. J. Multiphase Flow **16**, 323 (1990).
[7] D. Ma and G. Ahmadi, "A thermodynamical formulation for dispersed multiphase turbulent flows. II. Simple shear flows for dense mixtures," Int. J. Multiphase Flow **16**, 341 (1990).

[8] O. Simonin, "Continuum modeling of dispersed turbulent two-phase flows, Part 1: General model description," Technical Report, von Kármán Institute of Fluid Dynamics Lecture Series (1996).

[9] O. Simonin, "Continuum modeling of dispersed turbulent two-phase flows, Part 2: Model predictions and discussion," Technical Report, von Kármán Institute of Fluid Dynamics Lecture Series (1996).

[10] S. Sofiane (private communication, 2003).

[11] S. Sundaram and L. R. Collins, "A numerical study of the modulation of isotropic turbulence by suspended particles," J. Fluid Mech. **379**, 105 (1999).

[12] A. M. Ahmed and S. Elghobashi, "On the mechanisms of modifying the structure of turbulent homogeneous shear flows by dispersed particles," Phys. Fluids **12**, 2906 (2000).

[13] S. Elghobashi and G. C. Truesdell, "On the two-way interaction between homogeneous turbulence and dispersed solid particles. I. Turbulence modification," Phys. Fluids A **5**, 1790 (1993).

[14] M. Boivin, O. Simonin, and K. D. Squires, "Direct numerical simulation of turbulence modulation by particles in isotropic turbulence," J. Fluid Mech. **375**, 235 (1998).

[15] A. M. Ahmed and S. Elghobashi, "Direct numerical simulation of particle dispersion in homogeneous turbulent shear flows," Phys. Fluids **13**, 3346 (2001).

[16] F. Mashayek, D. B. Taulbee, "Statistics in particle-laden plane strain turbulence by direct numerical simulation," Int. J. Multiphase Flow **27**, 347 (2001).

[17] F. Mashayek, D. B. Taulbee, "Turbulent gas-solid flows. I. Direct simulations and Reynolds stress closures," Numer. Heat Transfer, Part B **41**, 1 (2002).

[18] A. Ferrante and S. Elghobashi, "On the physical mechanisms of two-way coupling in particle isotropic turbulence," Phys. Fluids **15**, 315 (2003).

[19] Q. Wang and K. D. Squires, "Large eddy simulation of particle laden turbulent channel flow," Phys. Fluids **8**, 1207 (1996).

[20] Q. Wang, K. D. Squires, and O. Simonin, "Large eddy simulation of turbulent gas-solid flows in a vertical channel and evaluation of second-order methods," Int. J. Heat Fluid Flow **19**, 505 (1998).

[21] B. Shotorban and F. Mashayek, "Modeling subgrid-scale effects on particles by approximate deconvolution," Phys. Fluids **17**, 081701 (2005).

[22] M. Boivin, O. Simonin, and K. D. Squires, "On the prediction of gas-solid flows with two-way coupling using large eddy simulation," Phys. Fluids **12**, 2080 (2000).

[23] Y. Xu, Master's thesis, Iowa State University, 2004.

[24] G. Ahmadi, "A two-equation turbulence model for compressible flows based on the second law of thermodynamics," J. Non-Equil. Thermodyn. **14**, 45 (1989).

[25] G. M. Pai and S. Subramaniam, "Analysis of turbulence models in Lagrangian-Eulerian spray computations," in Proceedings of the 17th Annual Conference on Liquid Atomization and Spray Systems, Intl. Liquid Atomization and Spray System Soc. ILASS (2004).

[26] A. A. Amsden, P. J. O'Rourke, and T. D. Butler, "KIVA–II: A computer program for chemically reactive flows with sprays," Technical Report, Los Alamos National Laboratory (1989).

[27] I. Kataoka, A. Serizawa, and T. Matsumoto, "Basic equations of turbulence in gas-liquid two-phase flow," Int. J. Multiphase Flow **15**, 843 (1989).

[28] D. A. Drew and S. L. Passman, *Theory of Multicomponent Fluids*, Vol. 135 of Applied Mathematical Sciences (Springer, New York, 1999).

[29] B. E. Launder, in *Simulation and Modeling of Turbulent Flows*, edited by M. H. T. B. Gatski and J. Lumley (Oxford University Press, New York, 1996), Chap. 6, pp. 243–310.

[30] D. C. Besnard and F. H. Harlow, "Turbulence in two-field incompressible flows," Technical Report LA-10187MS, Los Alamos National Laboratory, Albuquerque, NM (1985).

[31] B. Moses and C. Edwards, "LESS-type filtering and partly-resolved particles," in *Americas 18th Annual Conference on Liquid Atomization and Spray Systems* (ILASS, Irvine, CA, 2005).

[32] T. Fallon and C. B. Rogers, "Turbulence-induced preferential concentration of solid particles in microgravity conditions," Exp. Fluids **33**, 233 (2002).

[33] R. N. Parthasarathy and G. M. Faeth, "Turbulence modulation in homogeneous particle-laden flows," J. Fluid Mech. **220**, 485 (1990).

[34] U. Schumann, "Realizability of Reynolds-stress turbulence models," Phys. Fluids **20**, 721 (1977).

[35] G. Balzer, A. Boelle, and O. Simonin, "Eulerian gas-solid flow modelling of dense fluidized bed," in *Fluidization VIII*, International Symposium of Engineering Foundation, 1998, pp. 1125–1134.

[36] J. Cao and G. Ahmadi, "Gas-particle two-phase turbulent flow in a vertical duct," Int. J. Multiphase Flow **21**, 1203 (1995).